ACTA IMEKO
ISSN: 2221-870X
June 2025, Volume 14, Number 2, 1 - 11

Comparing marker-less vision systems for contact detection in wheelchair propulsion: Evaluating the limitations of angular speed difference

Enrico Ferlinghetti[1,2], Jelmer Braaksma[2], Thomas Rietveld[3], Han Houdijk[2], Riemer Vegter[2,3], Matteo Lancini[4]

[1] *DIMI, Università degli Studi di Brescia, Brescia, Italy*
[2] *Department of Human Movement Sciences, University Medical Center Groningen, University of Groningen, The Netherlands*
[3] *Peter Harrison Centre for Disability Sport, School of Sport, Exercise and Health Sciences, Loughborough, United Kingdom*
[4] *DSMC, Università degli Studi di Brescia, Brescia, Italy*

ABSTRACT
The objective of this study is to compare the error in detecting the start and end times of hand-wheel contact during wheelchair propulsion using two marker-less vision systems: ASD and MLVS. The first system, based on angular speed difference (ASD), relies only on the difference in angular speed between the hand and the wheel, calculated from RGB videos collected at 240 Hz. The angular speed of the hand was assessed using MediaPipe, a marker-less detection system, while the angular speed of the wheel was computed using a visual encoder operating on coloured tape positioned on the wheel and hand-rim in two configurations: hexagonal and incremental. The second system, MLVS, uses RGB-depth videos collected at 60 Hz and incorporates additional parameters, such as radial distance and normal position, to evaluate contact. The reference for contact initiation and termination was obtained from the torque signal collected on an instrumented wheelchair ergometer, with subsequent corrections made through expert visual inspection of video recordings. Data were collected from two participants who propelled a wheelchair on a wheelchair ergometer at 1.11 m/s and 0.21 W/kg body mass. Various thresholds for the angular speed difference between the hand and the wheel were tested, and the root mean square error (RMSE) for contact initiation and termination times was evaluated. The results showed that the lowest RMSE obtained with ASD was approximately 155 ms, while the RMSE obtained with MLVS were approximately 90 ms for contact initiation and 60 ms for contact termination, comparable to what was obtained with MLVS in previous studies. Accordingly, the study concludes that using only the relative angular speed between hand and hand-rim is not a reliable predictor of contact initiation or termination within the assessed experimental setup.

Section: RESEARCH PAPER

Keywords: Wheelchair; marker-less; vision system; contact detection

Citation: E. Ferlinghetti, J. Braaksma, T. Rietveld, H. Houdijk, R. Vegter, M. Lancini, Comparing marker-less vision systems for contact detection in wheelchair propulsion: Evaluating the limitations of angular speed difference, Acta IMEKO, vol. 14 (2025) no. 2, pp. 1-11. DOI: 10.21014/actaimeko.v14i2.2075

Section Editor: Andrea Scorza, University Roma Tre, Italy

Received February 18, 2025; **In final form** June 10, 2025; **Published** June 2025

Corresponding author: Enrico Ferlinghetti, e-mail: enrico.ferlinghetti@unibs.it

1. INTRODUCTION

Manual wheelchair propulsion is essential for daily activities and has a deep effect on the quality of life, health and social interaction of people who have lost their capability to walk [1], [2]. Optimisation of wheelchair design configurations is essential to minimise the risk of injury and increase the safety and independence of users [3]. Furthermore, with the increasing popularity of wheelchair sports such as tennis, basketball, and rugby, there is a growing emphasis on a more in-depth understanding of wheelchair propulsion and to further improve performance [4], [5], [6], [7].

The stroke cycle in wheelchair propulsion can be divided in two different phases: contact and recovery [8]. The contact phase can be further divided into coupling (or initial contact), pushing, and decoupling (or release) phases [8]. Coupling time is defined as the period between start of hand hand-rim contact and the application of a positive torque. Usually, during coupling time, the hand exerts a negative torque on the hand-

rim due to the different angular speeds of the two but in some cases the hand can approach the hand-rim with similar angular speed and therefore the negative torque is not recorded. Pushing time is further defined as the period in which the hand is applying a positive torque to the hand-rim [9]. Decoupling time is defined as the period between the end of the application of the positive torque and the end of the contact between the hand and the hand-rim. The duration of these phases can be used to evaluate the ergonomic benefits of different hand-rim designs or to track improvements during a rehabilitation or training process [10].

Pushing time can be evaluated according to the force or the torque applied by the user to the wheel, which can be measured using instrumented wheels [11], [12] or ergometers [13], [14] or inertial measurement units [15], [16], [17], while contact time, which corresponds to the total period in which the hand is in contact with the hand-rim is difficult to determine using the above-mentioned instruments since it is not always directly correlated to an exchange of forces between the hand and the hand-rim: the hand might approach it at the same speed without exerting any torque on it before the pushing phase.

A new approach to contact time detection is the use of a marker-less vision system based on a RGB-depth camera (MLVS), which has been presented and validated in [18], [19], showing a Root Mean Square Error (RMSE) in contact detection of approximately 60 ms, computed as the difference between the contact initiation and termination times estimated by the MLVS and the corresponding reference values. This result is better than the value of the quality of agreement obtained in [20] using inertial measurement units, which ranged between 20 ms and 330 ms, but, at the same time, as the RMSE can be used as an indicator of the uncertainty in contact times detection, the accuracy is still quite low when taking into account that the average push duration is approximately 300 ms [9]. The working principle of MLVS in contact time detection is based on the evaluation of the relative position between the hand and the hand-rim to compute several parameters, such as the radial and normal distance of the hand on the plane containing the hand-rim and the angular speed of the hand on the wheel's rotation axis. These parameters are then used to evaluate, for every sample, if the hand is touching the hand-rim. [21] carried out a Principal Component Analysis (PCA) on the parameters, showing that angular speed was one of parameters explaining most of the variance to define contact using MLVS, suggesting it might be a valid predictor of contact.

Accordingly, the current work aims to verify if angular speed alone, and, in particular, the angular speed difference (ASD) of the hand and the hand-rim on the rotation axis of the wheel, can be a good predictor of the contact between the two during wheelchair propulsion. Since the angular speed can be evaluated using the RGB images, this would allow to replace RGB-depth cameras with commercially available smartphone, as already suggested in [21], but also to simplify the understanding of this movement (as it would only be evaluated according to one parameter: the angular speed difference), making wheelchair contact detection more accessible and fostering the use of this parameter when assessing the performance of wheelchair users. Hence the research question of the current paper is: how do the ASD (in incremental and hexagonal configuration) and MLVS methods compare in accuracy in contact time detection with respect to visual inspection and qualitative assessment when tested on two able-bodied participants at standard testing speed of 1.11 m/s on an instrumented wheelchair ergometer? The testing speed of 1.11 m/s was chosen according to previous studies [22], [23].

Section 2 begins with the Materials sub-section, which describes the hardware used: an ergometer for collecting reference data, an iPhone for recording RGB frames, and a Realsense D435i for capturing RGB-depth images to run the MLVS contact detection algorithm. The Methods sub-section explains how the angular speed of the hand and hand-rim was determined from the iPhone recordings through MediaPipe for hand tracking and a visual encoder for the hand-rim and wheel. The Experimental Setup and Protocol sub-sections provide details on data collection, while the Reference Values sub-section elaborates on the manual data labelling procedure. Section 3 presents an analysis of the errors obtained when estimating contact initiation and termination times using ASD and MLVS with respect to the reference value. Section 4 discusses these results in depth, and finally, Section 5 concludes the paper by explaining why angular speed alone is insufficient for accurately determining contact times during wheelchair propulsion.

2. METHODOLOGY

2.1. Materials

An iPhone 11 (Apple, USA), collecting an RGB video with a resolution of 1920 × 1080 pixels and a frequency of 240 Hz, and a Realsense D435i, collecting frames for both the RGB and depth channel with a resolution of 848 × 480 pixels and a frequency of 60 Hz, were placed on the right side of the participant at approximately 1.2 m. The orientation of the cameras was parallel to the plane of the wheel, which had no camber angle. An example of the recorded image is shown in Figure 1.

The wheelchair (k-series, Küshall, Witterswil, Switzerland) was placed on an instrumented wheelchair roller ergometer (Esseda, Lode BV, The Netherlands) that collected torque exerted on each wheel and its speed at a frequency of 100 Hz. According to [13], the Root Mean Square Difference between the torque collected by this ergometer and an instrumented wheel, considered as gold standard, was of 0.18 Nm.

The technical specifications of the components (phone, RGB-depth camera and ergometer) are resumed in Table 1. The data collected were analysed using Python 3.9 with custom-written scripts.

Figure 1. Frame recorded by the high frequency camera. It is possible to notice the markers of coloured tape placed on the hand-rim (red and green) and on the wheel (yellow and blue).

Table 1. Experimental setup components with technical specifications

Component	Resolution, pixels	Acquisition Frequency, Hz	Data Acquired
iPhone 11	1920 x 1080 pixels	240	RGB images
Realsense D435i	848 x 480 pixels	60	RGB-depth images
Ergometer	NA	100	Torque and angular speed

2.2. Methods

The videos collected by the iPhone were used to identify the contact phases with the angular speed difference (ASD) method: the contact initiation and termination times were considered as the time corresponding to the first and last value in which the difference between the angular speeds of the hand and of the wheel was lower than a given threshold value. For comparison with another marker-less vision system contact detection method, contact times were also computed by MLVS, using the RGB-depth frames collected by the Realsense, as detailed in [18], [19], [21].

2.2.1. Hand's Angular Speed

The position of the hand was detected on the image plane in pixel coordinates using MediaPipe [24], an algorithm able to locate the position of 21 keypoints of the hand (4 for each finger and one for the wrist), already used to detect hand during wheelchair propulsion in [19], [21]. The coordinates of the centre of the hand were obtained as the average value of the x and y coordinates of the 21 keypoints. The angular position around the rotation axis of the wheel was smoothed using a 0.2 s-wide moving average filter: for each sample, the value was computed as the average of the values of all the data points within the sliding window centred on it, preserving the original sampling rate. Similarly, the angular speed was computed by fitting a linear regression model over a 0.1 s-wide sliding window centred at each time point: the slope of the regression line was taken as the instantaneous angular speed, also preserving the original sampling rate. The values of 0.2 s for the width of the moving average filter and of 0.1 s for the width of the linear regression were chosen after a qualitative analysis aimed to balancing the trade-off between noise removal and loss of information about rapid oscillations.

2.2.2. Wheel's Angular Speed

Angular position of the wheel was obtained using markers (pieces of tape) of approximately 2 cm of four different colours: red, green blue and yellow. Two markers' colours were placed on the hand-rim and two on the wheel, as shown in Figure 1. The angular speed of the wheel was calculated as the derivative of the angular position, obtained from the markers using the principle of a visual encoder [25] and cross-correlation. Assuming no relative motion between the hand-rim and the wheel, the angular speed was computed as the average of the two.

The procedure to obtain the angular position of the wheel and of the hand-rim according to the collected image was the following: the original image was acquired in the RGB domain and limited to detect the pixels corresponding to the four markers' colours, as shown in Figure 2. To ensure that adjacent pixels belonging to the same marker were grouped as a single entity, the detected regions were post-processed through iterative morphological operations: dilation (with a squared mask of 8-pixel edges) and erosion (with a squared mask of 5-pixel edges) were applied in sequence for four times each. This operation was then followed by blob analysis: the centroid of each detected marker was determined in pixel coordinates and mapped to its angular position relative to the centre of the wheel.

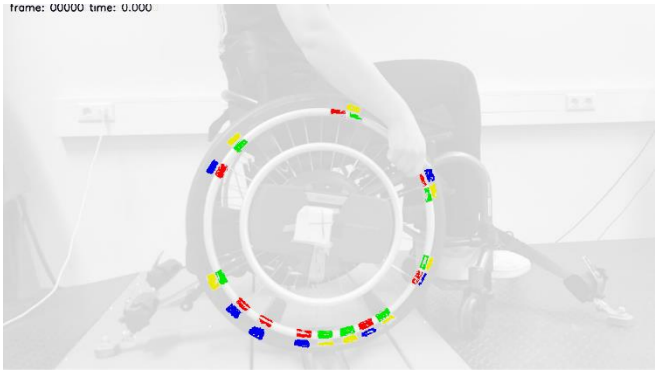

Figure 2. Frame recorded by the high frequency camera with highlight on the coloured markers detected by the RGB channels thresholding process. It is possible to notice that the blue marker on top is missing since it was not detected.

Two different configurations of marker placement were tested, as shown in Figure 3. In the first configuration, called "hexagonal", 6 markers of the same colour were placed at an equal distance of 60 deg from each other, as suggested in [26]. In the middle of the arc formed by each pair, another colour was placed, except for two consecutive arcs that were left empty to distinguish 0 deg position of the wheel and consequently its absolute rotation. Since the hand touching the hand-rim might obstruct some markers, a second configuration, called "incremental", was tested. In this case the distance between two successive markers was 1 deg higher than the distance of the previous pair, as expressed in equation (1), resulting in the following placement: 0 deg, 10 deg, 30 deg, 60 deg, 100 deg, 150 deg, 210 deg and 280 deg. The second colour was placed in the same way with a shift of 45 deg.

$$\theta_0 = 0 \text{ deg};\ \theta_1 = 10 \text{ deg};$$
$$\theta_n = \theta_{n-1} + (\theta_{n-1} - \theta_{n-2}) + 10 \text{ deg}. \quad (1)$$

Based on the angular positions of the detected markers, a signal ranging from 0 to 1 was generated. The signal was initially set to 0, with gaussian shaped peaks centred at the angular

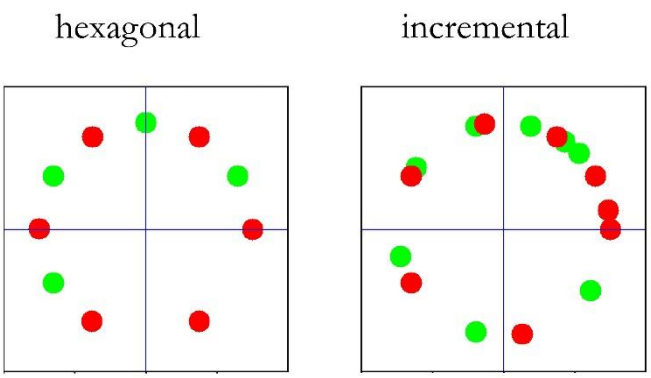

Figure 3. Example of the "hexagonal" and "incremental" configuration for the markers configuration on the hand-rim and on the wheel. In the figure only two colours are shown, but red, green, blue and yellow were used: two on the hand-rim and two on the wheel.

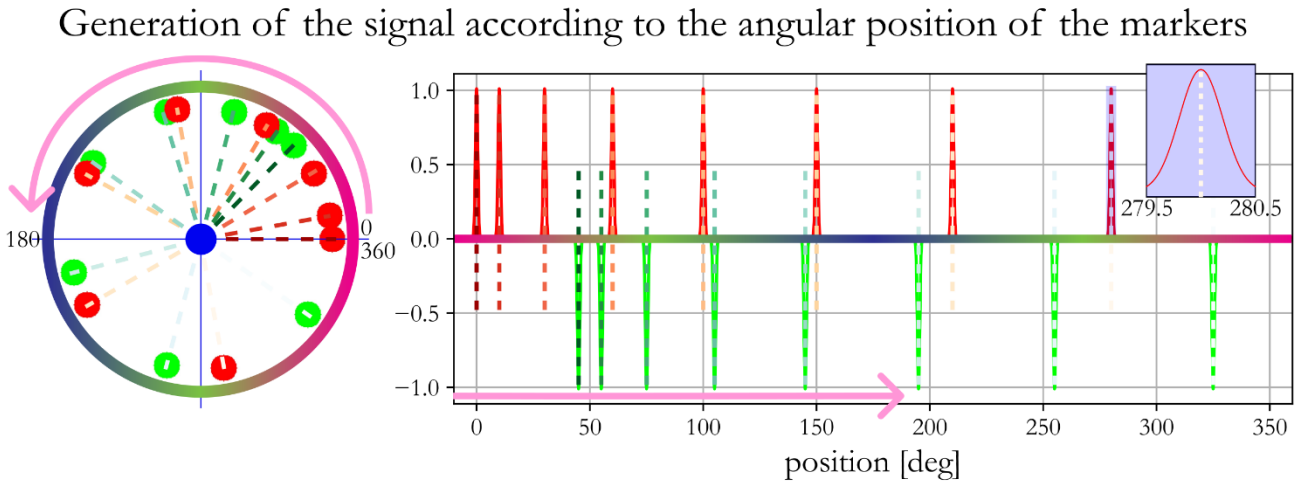

Figure 4. Example of how the signal for cross-correlation was generated: gaussian shaped peaks centred at the angular positions of the detected markers.

positions of the markers with a maximum value of 1. The standard deviation of each gaussian curve was approximately 0.2 deg, proportional to the amplitude of the corresponding pixel region. Signals were created separately for each of the two marker colours (two for the wheel and two for the hand-rim) and then subtracted, producing a new signal characterised by peaks at -1 or +1 at the positions of the respective markers, as shown in Figure 4. The phase shift of this signal was then computed using cross-correlation with a reference signal corresponding to the wheel at a known 0 deg position, as suggested in [27], [28], allowing for the determination of the wheel's angular position.

By repeating this process for each frame, the angular position of the wheel over time was obtained. As done for the hand, the resulting position signal was smoothed using a 0.2 s-wide moving average filter: for each sample, the value was computed as the average of the values of all the data points within the sliding window centred on it, preserving the original sampling rate. Similarly, the angular speed was computed by fitting a linear regression model over a 0.1 s-wide sliding window centred at each time point: the slope of the regression line was taken as the instantaneous angular speed, also preserving the original sampling rate. The width of 0.2 s and 0.1 s for the sliding windows were chosen, as done for the hand, to balance the trade-off between noise removal and loss of information about rapid oscillations.

Software simulations were carried out in Python, generating gaussian shaped peaks signals to assess which configuration type (hexagonal or incremental) was more robust against marker obstruction, incorrect marker identification, and angular position detection noise. For both configuration types, gaussian shaped peaks signals were generated. The number of peaks varied to simulate scenarios where markers were obstructed or incorrectly detected (ranging from 0 to 4). The peak positions were randomly shifted around their centres to simulate detection noise, with a shifting amplitude ranging from 0 deg to 20 deg in 2 deg increments. Each combination of obstructed markers, incorrectly detected markers, and peak position shifts due to noise was simulated 10 times for each angular position (from 0 deg to 350 deg in 10 deg increments), resulting in a total of 198000 records.

For each record, the difference between the reference and the angular position detected applying cross-correlation to the modified signal was computed.

2.2.3. Contact Detection with ASD

As shown in Figure 5, ASD considered the hand in contact with the hand-rim when the absolute value of the difference of the two angular speeds was lower than a certain threshold. Therefore, contact initiation and termination times were considered as the moments corresponding to the first and last value in which the difference was within a given threshold value. As shown in the figure, the angular speed of the wheel (which is kept at a constant speed of approximately 1.11 m/s by the participant that pushed it while receiving a real-time visual feedback about the speed) is approximately 200 deg/s. The hand angular speed ranges between -200 deg/s (during the recovery phase) and +200 deg/s (during the pushing phase). The threshold values were therefore tested between 20 deg/s and 400 deg/s with steps of 20 deg/s.

2.3. Experimental setup

The tests were carried out under standardised laboratory conditions with typical lighting of indoor environments and no focus or lighting to enhance hand recognition. Assistance for hand recognition was intentionally avoided to ensure the setup remained as replicable as possible and because it was unnecessary, as MediaPipe successfully recognised the hand even under normal lighting conditions. The hand needed to be placed within the camera's field of view, while the framing of the participant's face was not essential for MediaPipe to execute hand recognition. An ergometer was used to measure torque and wheel's angular velocity. The ergometer and the cameras were synchronised through cross-correlation, utilising the signal produced by each participant at the conclusion of each trial while pushing the wheel forward and backward three times, maintaining a firm grip on the hand-rim.

2.4. Experimental protocol

Two right-handed able-bodied participants (one for the hexagonal and one for the incremental configuration) performed 4 blocks of 4 min submaximal propulsion (1.11 m/s and 0.21 W/kg body mass, chosen according to [22]) after a 48 min practice period. A two-minute rest period preceded each block. Only the data from the last minute of one of the four tests of each subject were used. This choice was necessary since each minute of data collection consisted of approximately 10 GB. The last minute was chosen since the subject already reached a steady state condition, ensuring the speed was as stable as possible at 1.11 m/s. The study received approval from

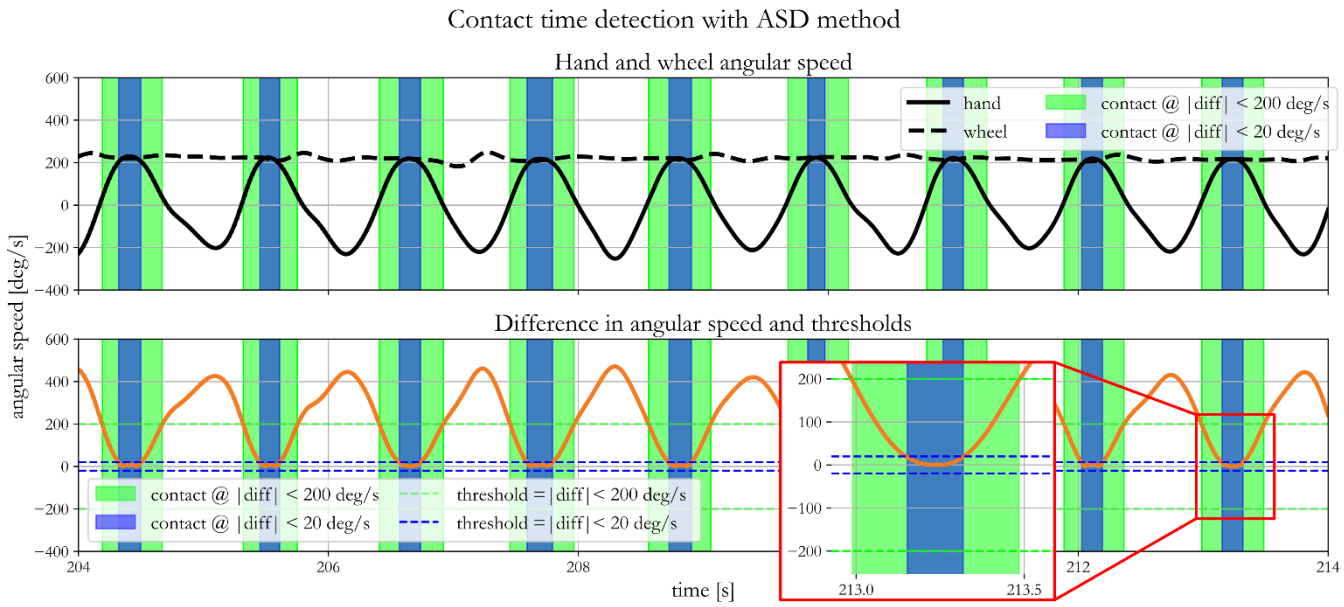

Figure 5. Example of the application of the ASD method for contact detection. The top subplot shows the angular speed of the hand (in solid line) and of the wheel (in dashed line) over time. The bottom subplot shows the absolute value of the difference between the two (in orange line) over time. When the difference is within the range of ±20 °/s or ±200 °/s (highlighted by the blue/green dashed lines), ASD considers the contact is occurring (highlighted by the blue/green rectangles).

the ethical committee at the University Medical Centre Groningen (Groningen, The Netherlands, reference number: 202100883).

2.5. Reference Value

The reference values for contact initiation and termination can be measured according to "the 3-dimensional external forces applied by the hand on the handrim" [9]. Since this method was never metrologically validated and the ergometer used for this study only collected the torque, which corresponds to the force applied only on the rotation axis and not the 3-dimensional forces, the reference value was obtained with a semiautomatic procedure composed of two steps to determine contact initiation and termination times.

Firstly, the algorithm filtered the torque signal with a low-pass 2nd order Butterworth filter with a cutoff frequency of 15 Hz and divided the torque by its standard deviation. Then the algorithm split the contact phase in its the three sub-phases [8], as shown in Figure 6:

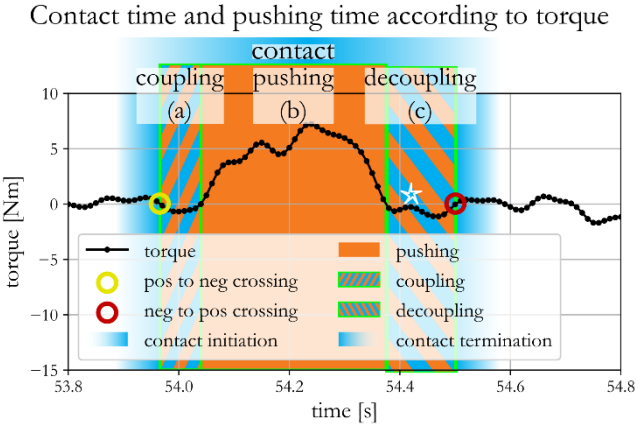

Figure 6. Example of one push with highlighted the contact phase and its sub-phases: coupling, pushing and decoupling. The positive-to-negative (yellow circle) and negative-to-positive (red circle) crossing were used to define the beginning of the coupling phase and the end of the decoupling phase. These moments were then manually corrected by an operator according to the video recordings.

1. Pushing phase ("b" in the figure), which is the period of positive torque application [9]. The algorithm detected the pushing phase as the period in which the torque was above a cutoff threshold of 0.2 Nm with at least one value above a minimum peak value of 1 Nm. This operation was executed using the "push_by_push" function of the Worklab package in Python [29], appositely developed for torque analysis.
2. Coupling phase ("a" in the figure), which is the period before the pushing phase in which the hand is touching the hand-rim exerting a negative torque due to different speeds between the two. The algorithm identified this phase as the period between the moment in which the torque crossed the zero value from positive to negative (yellow circle in the figure) and the beginning of the pushing phase.
3. Decoupling phase ("c" in the figure), which is specular to coupling phase at the end of the pushing phase. The algorithm identified this phase as the period between the end of the pushing phase and the moment in which the torque crossed the zero value from negative to positive (red circle in the figure). As shown in the same figure, a local peak in the torque signal can be observed during the decoupling phase (highlighted with a white star). In this case, the torque approached but did not exceed 0 Nm, and consequently, the algorithm did not identify this point as the end of the decoupling phase. In other contact events, depending on the participant's propulsion technique and the noise level, the peak was either absent, remained well below the 0 Nm threshold, or crossed the 0 Nm value and was thus detected by the algorithm as the end of the decoupling phase. This variability, as well as the noise signal, made necessary a manual intervention in most of the cases (>95%), executed by an operator who refined

the contact initiation and termination times indicated by the torque analysis according to the video recording. The manual refinement considered that the contact might have started before the positive-to-negative crossing that, according to the algorithm, defined the beginning coupling phase (in the white to cyan area of the figure) and the contact might have ended after the negative-to-positive crossing that, according to the algorithm, defined the end of decoupling phase (in the cyan to white are of the figure).

To evaluate the repeatability of the operator in identifying the contact phases, a second operator labelled the data and the difference between the contact initiation (and termination) times indicated by the two operators was evaluated. The root mean square of the difference resulted to be approximately 50 ms for both contact initiation and termination times.

2.6. Data Analysis

The comparison between hexagonal and incremental marker configurations was evaluated through both software simulations and real-data analysis. In the software simulations, the Root Mean Square Error (RMSE) in angular position detection was assessed. The analysis considered the configuration type (hexagonal and incremental) as a between-subject factor, while three within-subject factors were included: the number of obstructed markers (ranging from 0 to 4), the number of incorrectly detected markers (from 0 to 4), and the noise amplitude (from 0 deg to 20 deg in 2 deg increments). Each scenario was simulated 10 times at intervals of 10 deg (from 0 deg to 350 deg), yielding a total of 198000 records. The system was further validated by comparing the angular speed measured by the vision system with that recorded by the ergometer during subject trials.

The accuracy of contact detection was assessed by comparing both the ASD method and the MLVS approach to a reference value, which was obtained through a semi-automatic procedure analysing the torque signal and manually refining contact initiation and termination times using video recordings. For both ASD and MLVS methods, the difference between the contact initiation and termination times were subtracted to the respective reference values. These differences were treated as errors and consequently the RMSE, the mean errors and standard deviations were computed to quantify their accuracy. For ASD, the errors were analysed across different angular speed difference thresholds, with the optimal threshold identified for each marker configuration (hexagonal and incremental) and for contact initiation, termination and duration. For MLVS, contact initiation and termination times were determined using RGB-depth data, and RMSE, mean errors and standard deviations were computed as the difference from the reference values to assess detection accuracy.

3. RESULTS

3.1. Markers' Configuration

The software simulation comparing the hexagonal and incremental configurations revealed a difference in the RMSE between the two with respect to all the within-subject factors (obstructed markers, wrongly detected markers, and noise amplitude). Figure 7 shows the RMSE values for both configurations across different levels of misdetected markers and noise amplitude. Focusing on the sharp lines, which correspond to the scenario with no misdetected markers, it was

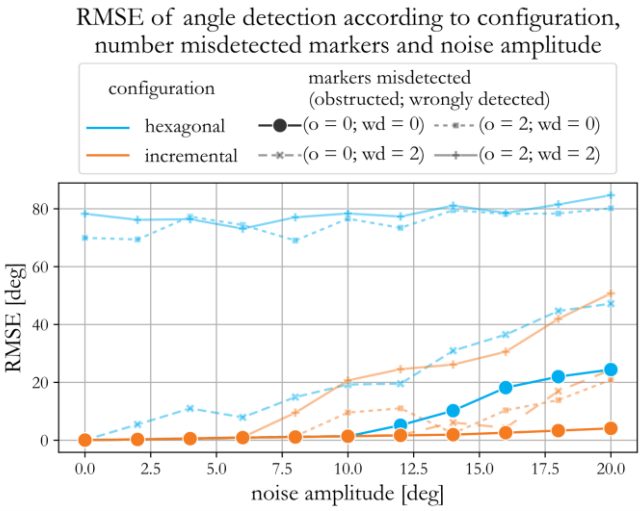

Figure 7. Root Mean Square Error (RMSE) of angular position obtained during software simulations between the two markers configuration: hexagonal (in cyan) and incremental (in orange) according to the number of obstructed and wrongly detected markers (from 0 to 4 in the simulations, in the figure only shown the cases with 0 and 2 markers) and, on the x axis, the noise level (from 0 deg to 20 deg).

observed that RMSE increased with noise amplitude for both configurations. However, the hexagonal configuration was significantly more sensitive to noise, with RMSE values exceeding 20 deg when the noise amplitude exceeded 18 deg. Conversely, the incremental configuration maintained a much lower RMSE (approximately 4 deg even at the highest noise amplitude of 20 deg). For the cases involving obstructed or misdetected markers (shown by the faded lines), the incremental configuration showed a greater robustness. When two markers were obstructed, the RMSE for the hexagonal configuration was around 70 deg, indicating a marked degradation in accuracy while in the incremental configuration, only a low increase in RMSE was observed under the same conditions.

3.2. Wheel's Angular Speed

The comparison between the angular speed of the wheel measured by the vision system and the reference value obtained by the ergometer revealed differences in accuracy between the two marker configurations opposite to those expected when considering the results of the simulation. The RMSE for the hexagonal configuration was 1.7 deg/s while for the incremental configuration was 11 deg/s. Figure 8 shows a ten-second recording, illustrating that the higher RMSE observed in the incremental configuration is a result of more prominent peaks in both the negative and positive directions. The negative

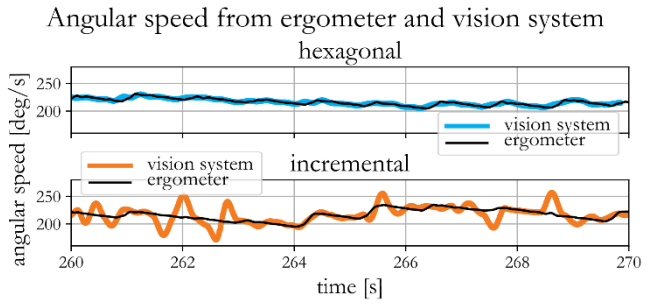

Figure 8. Angular speed recorded by the vision system (for the hexagonal configuration in cyan and for the incremental configuration in orange) and by the ergometer (in black) over time.

peaks occurred when the hand coupled with the hand-rim, exerting a negative torque that caused deceleration and a reduction in angular speed. The positive peaks occurred when the hand exerted a positive torque, leading to acceleration and an increase in angular speed.

3.3. Contact Detection with ASD

Figure 9 shows the RMSE, mean errors, and standard deviations for contact initiation and termination times according to the angular speed difference (ASD) method for the tested threshold values (20-400 deg/s) and according to MLVS method.

The analysis of the mean error for contact initiation showed that for lower threshold values the mean error was positive, indicating that the ASD method detected contact initiation later than the reference. Conversely, for higher thresholds, the mean error became negative, meaning that ASD detected contact initiation too early. This trend was clear in the incremental configuration but not in the hexagonal configuration, where the mean error remained consistently positive. Similarly, for contact termination, the mean error was negative at lower thresholds, suggesting that ASD anticipated the end of contact before the reference. As the threshold increased, the mean error became positive, indicating that ASD detected contact termination later than the reference.

For ASD, the RMSE were comparable for the two marker placement configurations, with a mean value of approximately 155 ms. As resumed in Table 2 for the contact initiation times, the minimum value of the RMSE for the hexagonal configuration was 140 ms, obtained when the difference between the angular speeds was 380 deg/s, while for the incremental configuration the minimum value of the RMSE was 190 ms, obtained when the difference between the angular speeds was 200 deg/s. For the contact termination times, the minimum value of the RMSE for the hexagonal configuration was 130 ms, obtained when the difference between the angular speeds was 140 deg/s, while for the incremental configuration the minimum value of the RMSE was 180 ms, obtained when the difference between the angular speeds is 120 deg/s.

The error of ASD in contact duration estimation was analysed as well, as shown in Figure 10 and in the last two rows of Table 2. The analysis of the mean error showed that, for both configurations, the contact durations were shorter than the reference value at lower thresholds and longer at higher thresholds. Regarding the RMSE, a notable difference emerged between the two configurations: the hexagonal method showed an RMSE of 81 ms, while the incremental configuration showed a higher RMSE of 250 ms. These values were obtained for similar angular speed differences, with 220 deg/s for the hexagonal configuration and 180 deg/s for the incremental configuration.

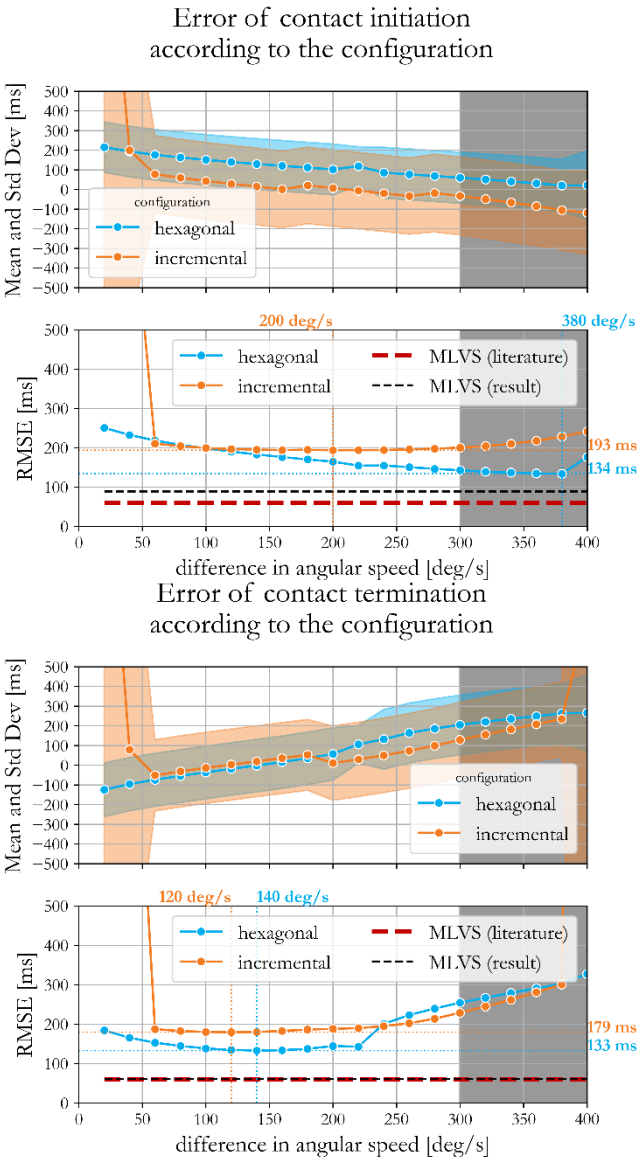

Figure 9. Mean, Standard Deviation and Root Mean Square Error (RMSE) of contact initiation and termination times computed with ASD according to the the two markers configuration: hexagonal (in cyan) and incremental (in orange). The minimum values of the RMSE in ms and the corresponding difference in angular speed are highlighted in dotted lines. Dashed lines show the RMSE obtained with MLVS for comparison. The red line represents the value of the RMSE obtained in [19], equal to 0.060 s while the black line represents the value of the RMSE obtained with the data collected in this study (89 ms for contact initiation and 61 ms for contact termination). The values of angular speed difference above 300 deg/s are shadowed in black since the values in this range are not considered reliable for threshold selection: the wheel moves at 200 deg/s and a difference in angular speed of 300 deg/s would mean that the hand is moving at half of the speed of the wheel in the opposite direction.

Table 2. Mean, Standard Deviation and Root Mean Square Error (RMSE) of contact initiation, termination and duration between ASD and the reference value according to the configuration (hexagonal and incremental). The values are only shown for the value of angular speed difference providing the lowest RMSE.

Contact event	Configuration	μ error, ms	σ error, ms	RMSE, ms	Angular Speed Difference, deg/s
Start	Hexagonal	21	130	130	380
Start	Incremental	7	190	190	200
End	Hexagonal	-2	133	130	140
End	Incremental	3	180	180	120
Duration	Hexagonal	-12	81	81	220
Duration	Incremental	30	250	250	180

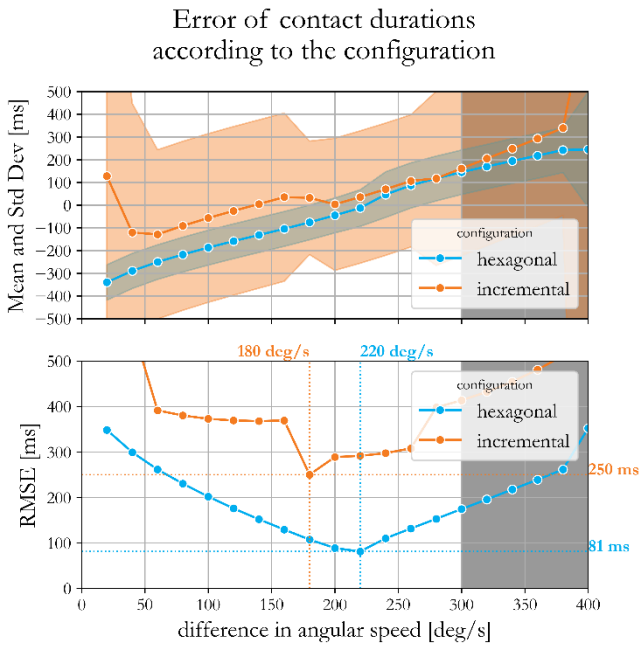

Figure 10. Mean, Standard Deviation and Root Mean Square Error (RMSE) of contact duration times computed with ASD according to the two markers configuration: hexagonal (in cyan) and incremental (in orange). The minimum values of the RMSE in ms and the corresponding difference in angular speed are highlighted in dotted lines. The values of angular speed difference above 300 deg/s are shadowed in black since the values in this range are not considered reliable for threshold selection.

3.4. Contact Detection with MLVS

For MLVS, the RMSE obtained was 89 ms for the contact initiation times and 61 ms for the contact termination phases. As shown in Table 3, since the value of 89 ms was slightly higher than the value of RMSE equal to 60 ms obtained in [18], [19], [21], also the mean and the standard deviation of the errors were investigated. The mean error in contact start of 69 ms indicates that MLVS is detecting the initiation of the contact later than the reference value while the contact start of -18 ms indicates that MLVS is detecting the termination of the contact slightly before the reference value. The standard deviations of the errors of both contact initiations and terminations are comparable with those presented in literature [18], [19], [21].

4. DISCUSSION

The objective of this study was to assess whether the angular speed difference (ASD) between the hand and the hand-rim could reliably predict contact times during manual wheelchair propulsion. Specifically, the study aimed to compare the accuracy of ASD, which relies solely on angular speed difference, in both incremental and hexagonal configurations, with that of the marker-less vision system (MLVS), which incorporates additional parameters such as radial and normal positions and speeds. The comparison was made by evaluating the errors relative to a reference value obtained through a semi-automatic process that analysed torque signals and manually refined contact initiation and termination times using video recordings. If ASD demonstrated consistent behaviour across the two subjects and configurations at a speed of 1.11 m/s, it would suggest that ASD could be a reliable predictor at least at that speed. However, the results revealed inconsistent performance of ASD between the two subjects and higher RMSE values compared to MLVS, proving that angular speed alone is not sufficient for accurate contact detection during wheelchair propulsion within the assessed experimental setup.

Table 3. Mean, Standard Deviation and Root Mean Square Error (RMSE) of contact initiation and termination times between MLVS and reference value.

Contact event	μ error, ms	σ error, ms	RMSE, ms
Start	69	43	89
End	-18	56	61

4.1. Markers' Configuration

Software simulations were carried out to compare the two possible configurations of coloured markers on the wheel and on the hand-rim (hexagonal and incremental). The two configurations were tested according to the number of misdetected (obstructed and wrongly detected) markers and according to the noise amplitude introduced in the angular position of each marker. The results, depicted in Figure 7, showed that the incremental configuration was more robust to both marker misdetection and noise amplitude. This can be justified considering that in the incremental configuration, if one or more markers are obstructed or missing, the angular position of the wheel can still be determined using the remaining markers, due to the increasing angular distance between successive markers. In contrast, the hexagonal configuration requires all markers to be present and properly detected to calculate the angular position. Regarding noise, the closer spacing of the first three markers in the incremental configuration (0 deg, 10 deg, and 30 deg) can cause the gaussian curves to overlap, leading to potential noise superimposition and reduced accuracy in angular position detection. However, as the distance between the markers increases (150 deg, 210 deg and 280 deg), the configuration becomes more robust to noise, as the larger distances reduce the risk of noise affecting adjacent markers. On the other hand, in the hexagonal configuration, the 60 deg distance between markers of the same colour is wide enough to minimise overlap of gaussian curves, but all the markers are equally susceptible to the same noise shifts, which can affect the overall accuracy of angular position detection.

4.2. Wheel's Angular Speed

While the incremental configuration showed a clear advantage in robustness during software simulations, the hexagonal configuration showed a better performance in terms of angular speed accuracy when comparing the vision system measurements to the ergometer reference on the data collected from the two participants. The hexagonal configuration showed a smaller RMSE (1.7 deg/s) compared to the incremental configuration (11 deg/s) in angular speed detection. Since the incremental configuration was more robust and accurate in the simulations, it is possible that the peaks observed in the incremental configuration (responsible of the higher RMSE) were actually occurring but have been smoothed when the angular speed was recorded by the ergometer. This smoothing effect could be due to mechanical filtering resulting from the interaction between the wheel and the roller (which is not captured by the vision system) and the low-pass filter applied in the ergometer, which reduces high-frequency noise and fluctuations in the recorded data. This aspect was not further investigated since the focus of the study was not the validation of the angular speed detection but the contact times detection during wheelchair propulsion using the difference of angular speed between hand and hand-rim.

4.3. Contact Detection with ASD

Contact time detection with ASD method was validated against a reference value obtained through torque analysis and manual correction. For comparison, another marker-less vision system method for contact times detection, MLVS, which has a standard uncertainty of 60 ms [19], was carried out on the same data. The results assessed that using the ASD method led to higher RMSE values in contact initiation and termination detection times compared to MLVS.

Regarding ASD, the lowest RMSE obtained for contact initiation was 140 ms for hexagonal configuration and 190 ms for incremental configuration, while for contact termination, the lowest RMSE obtained was 130 ms for hexagonal configuration and 180 ms for incremental configuration. Furthermore, the lowest RMSE values for contact initiation were obtained at different angular speed difference thresholds: 380 deg/s for hexagonal configuration and 200 deg/s for incremental configuration while the lowest RMSE values for contact termination were obtained at similar angular speed difference thresholds: 140 deg/s for hexagonal configuration and 120 deg/s for incremental configuration. The variability of thresholds for contact initiation suggests that there is no single optimal threshold that reliably defines the contact initiation phase across different propulsion cycles and subjects. In addition, a threshold of 380 deg/s for contact initiation appears highly unrealistic, considering that during propulsion, as shown in Figure 5, the wheel itself moves at approximately 200 deg/s. At a threshold of 380 deg/s, the hand would be moving at nearly the same speed as the wheel but in the opposite direction, which is not a plausible scenario for the actual moment of contact. This further supports the idea that ASD alone is not a reliable predictor for contact initiation.

The analysis of the mean error values of ASD showed that for contact initiation the mean error was positive at lower thresholds, indicating a delayed detection of the event, and became negative at higher thresholds, denoting an early detection. Conversely, for contact termination, the mean error was negative at lower thresholds, indicating an early detection of the contact end, and became positive at higher thresholds, implying a delayed detection.

Furthermore, an analysis of the estimated contact durations revealed that for lower thresholds, the detected contact phases were generally shorter than the reference values, whereas for higher thresholds, they were overestimated. This pattern was consistent across both the hexagonal and incremental configurations while the RMSE were different: 250 ms for incremental configuration and 81 ms for hexagonal.

4.4. Comparison of Contact Detection with ASD and MLVS

The RMSE obtained with ASD were considerably higher than those obtained with MLVS, which reported an RMSE of 89 ms for contact initiation and 61 ms for contact termination, comparable to the value of 60 ms obtained in [19]. On the other hand, in this study the mean value of the error in contact initiation time detection highlighted a systematic effect: MLVS was 69 ms late in predicting the start of the contact, which could be due to differences in the technique of the two tested participants. Nonetheless, the RMSE obtained with the MLVS contact detection method in this study are comparable to those reported in previous works, such as [19], reinforcing the robustness and repeatability of MLVS when applied to wheelchair contact detection on an ergometer.

The discrepancy in performance between ASD and MLVS highlights the limitations of using angular speed difference alone as a predictor of contact times. The main reason for this discrepancy is that angular speed difference does not account the complex interaction between the hand and the hand-rim during wheelchair propulsion: contact starts as the hand approaches the hand-rim, continues as long as the hand is firmly gripping the hand-rim (and the two are therefore moving at the same angular speed along the wheel's rotation axis) and ends when the hand detaches from the hand-rim. This can be better explained by additional kinematic parameters considered by MLVS, such as radial position, radial speed and angular acceleration, which can be obtained from simple RGB images, as explained in [21], but also from normal position and normal speed, which require also the depth information to be computed, as explained in [19]. Such parameters are not accounted for when using ASD, which relies solely on angular speed difference.

Moreover, since during the pushing phase the hand maintains a firm grip on the hand-rim, the evaluation of angular speed difference might be useful for detecting the pushing phase itself rather than the moments of contact initiation and termination. However, the pushing phase can already be detected using ergometers and instrumented wheels, as it corresponds to the application of a positive torque on the hand-rim.

4.5. Study Limitations

The small sample size, as data were collected from only two participants, might be considered a limitation of this study. However, despite the limited dataset, the ASD method showed consistently high RMSE values across both participants while MLVS provided results comparable to those found in the literature. Accordingly, the observed discrepancies in ASD performance are more likely due to limitations of the method itself rather than an insufficient number of participants. For this reason, further investigation with a larger participant pool was not pursued, as it was unlikely to yield substantially different findings. Additionally, manual data labelling for ground truth contact times was a time-consuming process, making large-scale analysis quite difficult.

Regarding the manual labelling process, inter-operator uncertainty was not considered when evaluating errors in contact detection. This decision was taken according to the fact that the differences in contact initiation and termination times between the operator that labelled the data and the second one, used as a comparison, resulted in a root mean square difference of 50 ms. This difference was smaller than the RMSE between the operator's annotations and the times indicated by ASD (average RMSE of 160 ms) and indicated by MLVS (average RMSE of 75 ms). Additionally, the difference of 50 ms between the two operators was not further investigated in the current work since the focus was on the comparison between ASD and MLVS methods. Nonetheless, the difference between the two operators obtained in the present study should be taken into account in future studies aimed at improving the accuracy of contact detection method since, in that case, the inter-operator uncertainty (of 50 ms in the current work) and the uncertainty of the contact measuring device compared to the ground truth (lower than the 75 ms obtained for MLVS in the current work) might become comparable.

A limitation of this study consists in the lack of validation of the hand's angular speed detection. Since no reference system

was available to directly measure the hand's angular speed, potential inaccuracies in its estimation could have influenced the results, further contributing to the observed discrepancies in ASD performance. It is also important to consider that MLVS incorporates angular speed as one of its parameters to evaluate contact detection.

Another limitation lies in the threshold selection for angular speed difference, which was tested from 20 deg/s to 400 deg/s with steps of 20 deg/s from with increments of 20 deg/s. This relatively large step size may have prevented the identification of a more precise threshold for contact detection. However, given the already suboptimal performance observed with ASD, refining the threshold step size was unlikely to yield substantial improvements. Therefore, the larger step size, while a limiting factor, did not significantly affect the overall conclusions of the study.

A third limitation might be the choice of window widths for the moving average filter (0.2 s) and linear regression (0.1 s). These values were selected arbitrarily based on a qualitative evaluation that balanced noise reduction while preserving rapid oscillations. This qualitative approach was preferred over a quantitative analysis, which might have identified a more optimal combination of window widths, since the selected widths were sufficient to achieve satisfactory results and a quantitative analysis was considered unnecessary, as it would not have significantly improved the measurement outcome.

This study only examined a single propulsion speed (1.11 m/s), which may have restricted the generalizability of the results. If multiple speeds had been analysed, it is likely that the optimal thresholds would have varied to an even greater extent, further underscoring the inconsistency of using angular speed difference alone for contact detection.

5. CONCLUSIONS

This study evaluated the feasibility of using angular speed difference (ASD) between hand and hand-rim as a standalone predictor for detecting contact initiation and termination in manual wheelchair propulsion. Previous research on the MLVS approach demonstrated reliable contact detection using RGB-depth data [18], [19] and later simplified the method to rely solely on RGB images, achieving comparable accuracy [21]. Principal Component Analysis (PCA) applied to MLVS data identified angular speed of the hand as one of the most significant features for contact detection [21], leading to the hypothesis that ASD alone could serve as a viable alternative. However, the results of this study indicate that ASD is not sufficient for accurate contact detection, as it led to higher RMSE values compared to MLVS and exhibited inconsistencies in threshold optimization across the two tested subjects, confirming that this simplification results in a loss of accuracy. Possibly, the ASD method could be useful only for detecting the pushing phase rather than contact initiation and termination. However, this information is already readily available from ergometers and instrumented wheels, as the pushing phase corresponds to a positive torque application.

As already demonstrated in [21], incorporating additional parameters such as radial distance, radial speed, and angular acceleration improves contact detection when using only RGB data, which can still be collected with commercially available smartphones, achieving results comparable to those obtained when normal distance and speed are also considered with depth information. The findings of this study reinforce the need for a more comprehensive approach that considers multiple motion features rather than relying solely on angular speed difference, aiming to reduce the standard uncertainty in contact time detection of 60 ms, which is not yet satisfactory but paves the way for a more accurate and reliable marker-less visions system method for wheelchair propulsion analysis.

AUTHORS' CONTRIBUTION

Conceptualization: EF, RV, ML; Data curation: EF, ML; Formal Analysis: EF, RV, ML; Funding acquisition: HH, RV Investigation: JB; Methodology: EF, TR, ML; Project administration: HH, RV, ML; Software: EF, JB; Resources: HH, RV; Supervision: HH, RV, ML; Validation: EF, ML; Visualization: EF, JB, TR; Writing – original draft: EF; Writing – review & editing: EF, JB, TR, HH, RV, ML.

REFERENCES

[1] M. T. Leving, R. J. K. Vegter, W. H. K. de Vries, S. de Groot, L. H. V. van der Woude, Changes in propulsion technique and shoulder complex loading following low-intensity wheelchair practice in novices, PLoS One, vol. 13, no. 11, Nov. 2018. DOI: 10.1371/journal.pone.0207291

[2] S. J. Briley, R. J. K. Vegter, V. L. Goosey-Tolfrey, B. S. Mason, The longitudinal relationship between shoulder pain and altered wheelchair propulsion biomechanics of manual wheelchair users, J. Biomech., vol. 126, Sep. 2021, 110626. DOI: 10.1016/j.jbiomech.2021.110626

[3] G. Bertolaccini, F. Sandnes, I. Filho, L. Paschoarelli, F. Medola, A descriptive study on the influence of wheelchair design and movement trajectory on the upper limbs' joint angles, in Advances in Intelligent Systems and Computing, Springer Verlag, 2018, pp. 645–651. DOI: 10.1007/978-3-319-60582-1_64

[4] R. J. F. Janssen, S. de Groot, L. H. V. Van der Woude, H. Houdijk, V. L. Goosey-Tolfrey, R. J. K. Vegter, Force–velocity profiling of elite wheelchair rugby players by manipulating rolling resistance over multiple wheelchair sprints, Scand. J. Med. Sci. Sport., 33, 8, Aug. 2023, pp. 1531-1540. DOI: 10.1111/sms.14384

[5] A. Iturricastillo, J. Sanchez-Grau, G. Carmona, A. García-Fresneda, J. Yanci, Initial Maximum Push-Rim Propulsion and Sprint Performance in Elite Men's Wheelchair Basketball, Int. J. Sports Physiol. Perform., vol. 19, no. 2, 2024, pp. 127–132. DOI: 10.1123/ijspp.2023-0206

[6] J. W. Chow, W. S. Chae, Kinematic analysis of the 100-m wheelchair race, J. Biomech., vol. 40, no. 11, Jan. 2007, pp. 2564–2568. DOI: 10.1016/J.JBIOMECH.2006.12.003

[7] T. Rietveld, R. J. K. Vegter, L. H. V. der Woude, S. de Groot, The interaction between wheelchair configuration and wheeling performance in wheelchair tennis: a narrative review, 2021, Routledge Sports Biomechanics, Volume 23, 2024, Issue 3, pp. 370–391. DOI: 10.1080/14763141.2020.1840617

[8] A. M. Kwarciak, S. A. Sisto, M. Yarossi, R. Price, E. Komaroff, M. L. Boninger, Redefining the Manual Wheelchair Stroke Cycle: Identification and Impact of Nonpropulsive Pushrim Contact, Arch. Phys. Med. Rehabil., vol. 90, no. 1, Jan. 2009, pp. 20–26. DOI: 10.1016/j.apmr.2008.07.013

[9] R. J. K. Vegter, J. Hartog, S. de Groot, (+ another 5 authors), Early motor learning changes in upper-limb dynamics and shoulder complex loading during handrim wheelchair propulsion, J. Neuroeng. Rehabil., vol. 12, no. 1, Mar. 2015, 26. DOI: 10.1186/s12984-015-0017-5

[10] T. Rietveld, R. J. F. Janssen, L. H. V. van der Woude, R. J. K. Vegter, S. de Groot, The Effect of a Newly Developed Hand Rim on Mobility Performance and Propulsion Technique in

Wheelchair Tennis Players, Int. J. Sports Physiol. Perform., Volume 19, Issue 11, Sep. 2024, pp. 1343–1346.
DOI: 10.1123/IJSPP.2023-0492

[11] F. Chénier, J. P. Pelland-Leblanc, A. Parrinello, E. Marquis, D. Rancourt, A high sample rate, wireless instrumented wheel for measuring 3D pushrim kinetics of a racing wheelchair, Med. Eng. Phys., vol. 87, Jan. 2021, pp. 30–37.
DOI: 10.1016/J.MEDENGPHY.2020.11.008

[12] L. Guo, A. M. Kwarciak, R. Rodriguez, N. Sarkar, W. M. Richter, Validation of a Biofeedback System for Wheelchair Propulsion Training, Rehabil. Res. Pract., Vol. 2011, 2011, pp. 1–7.
DOI: 10.1155/2011/590780

[13] R. De Klerk, R. J. K. Vegter, H. E. J. Veeger, L. H. V. Van Der Woude, Technical Note: A Novel Servo-Driven Dual-Roller Handrim Wheelchair Ergometer, IEEE Trans. Neural Syst. Rehabil. Eng., vol. 28, no. 4, Apr. 2020, pp. 953–960.
DOI: 10.1109/TNSRE.2020.2965281

[14] F. Chenier, P. Bigras, R. Aissaoui, A new wheelchair ergometer designed as an admittance-controlled haptic robot, IEEE/ASME Trans. Mechatronics, vol. 19, no. 1, Feb. 2014, pp. 321–328.
DOI: 10.1109/TMECH.2012.2235079

[15] V. G. de Vette, D. J. Veeger, M. P. van Dijk, Using Wearable Sensors to Estimate Mechanical Power Output in Cyclical Sports Other than Cycling - A Review, Sensors, vol. 23, no. 1, Jan. 2023, 50.
DOI: 10.3390/S23010050

[16] M. P. van Dijk, R. M. A. van der Slikke, R. Rupf, M. J. M. Hoozemans, M. A. M. Berger, D. J. H. E. J. Veeger, Obtaining wheelchair kinematics with one sensor only? The trade-off between number of inertial sensors and accuracy for measuring wheelchair mobility performance in sports, J. Biomech., vol. 130, Jan. 2022, 110879.
DOI: 10.1016/j.jbiomech.2021.110879

[17] M. P. van Dijk, M. Kok, M. A. M. Berger, M. J. M. Hoozemans, D. J. H. E. J. Veeger, Machine Learning to Improve Orientation Estimation in Sports Situations Challenging for Inertial Sensor Use, Front. Sport. Act. Living, vol. 3, Aug. 2021, Article 670263, 12 pp.
DOI: 10.3389/fspor.2021.670263

[18] E. Ferlinghetti, I. Salzmann, M. Ghidelli, T. Rietveld, R. Vegter, M. Lancini, Algorithm Development for Contact Identification during Wheelchair Tennis Propulsion using Marker-less Vision System, 2023 IEEE Int. Symposium on Medical Measurements and Applications, MeMeA 2023, Jeju, Republic of Korea, 14-16 June 2023, pp. 1-6.
DOI: 10.1109/MeMeA57477.2023.10171886

[19] E. Ferlinghetti, I. Salzmann, M. Ghidelli, T. Rietveld, R. Vegter, M. Lancini, Validation of Contact Measurement System for Wheelchair Tennis Propulsion using Marker-less Vision System, IEEE Trans. Instrum. Meas., Dec. 2023, 5006310, pp. 1–10.
DOI: 10.1109/tim.2023.3347811

[20] A. R. Lewis, D. S. Haydon, E. J. Phillips, (+ another 5 authors), Placement effects of inertial measurement units on contact identification in wheelchair racing, Sport. Biomech., vol. 20, no. 1, 2021, pp. 55–70.
DOI: 10.1080/14763141.2018.1522367

[21] E. Ferlinghetti, J. Braaksma, R. Vegter, M. Lancini, Marker-less Vision System Based on RGB Camera for Wheelchair Tennis Contact Detection, 2024 IEEE Int. Symp. on Medical Measurements and Applications (MeMeA), Eindhoven, Netherlands, 26-28 June 2024, pp. 1–6.
DOI: 10.1109/MeMeA60663.2024.10596820

[22] J. Braaksma, E. Ferlinghetti, S. de Groot, M. Lancini, H. Houdijk, R. J. K. Vegter, Calibration to Differentiate Power Output by the Manual Wheelchair User from the Pushrim-Activated Power-Assisted Wheel on a Force-Instrumented Computer-Controlled Wheelchair Ergometer, Actuators, vol. 13, no. 7, July 2024, p. 257.
DOI: 10.3390/act13070257

[23] T. Rietveld, R. J. K. Vegter, L. H. V. van der Woude, S. de Groot, A newly developed hand rim for wheelchair tennis improves propulsion technique and efficiency in able-bodied novices, Appl. Ergon., vol. 104, Oct. 2022, 103830.
DOI: 10.1016/j.apergo.2022.103830

[24] F. Zhang, V. Bazarevsky, A. Vakunov, A. Tkachenka, G. Sung, C.-L. Chang, M. Grundmann, MediaPipe Hands: On-device Real-time Hand Tracking, Jun. 2020, arXiv:2006.10214.
DOI: 10.48550/arXiv.2006.10214

[25] H. Kim, Y. Yamakawa, T. Senoo, M. Ishikawa, Visual encoder: robust and precise measurement method of rotation angle via high-speed RGB vision, Optics Express Vol. 24, Issue 12, 2016, pp. 13375-13386.
DOI: 10.1364/OE.24.013375

[26] R. Furferi, L. Governi, Y. Volpe, M. Carfagni, Design and assessment of a machine vision system for automatic vehicle wheel alignment, Int. J. Adv. Robot. Syst., vol. 10, May 2013, 5, 10 pp.
DOI: 10.5772/55928

[27] L. Iafolla, L. Witthauer, A. Zam, G. Rauter, P. C. Cattin, Proof of principle of a novel angular sensor concept for tracking systems, Sensors Actuators, A Phys., vol. 280, Sep. 2018, pp. 390–398.
DOI: 10.1016/j.sna.2018.08.012

[28] L. Iafolla, M. Filipozzi, S. Freund, A. Zam, G. Rauter, P. C. Cattin, Machine learning-based method for linearization and error compensation of a novel absolute rotary encoder, Meas. J. Int. Meas. Confed., vol. 169, Feb. 2021, 108547.
DOI: 10.1016/j.measurement.2020.108547

[29] R. de Klerk, Worklab: a wheelchair biomechanics mini-package, 2019, Version 1.0.0, File 5.9 MB.
DOI: 10.5281/ZENODO.3268671